AGU PUBLICATIONS

Geophysical Research Letters

RESEARCH LETTER

10.1002/2015GL067598

Key Points:

- Rays of seismic waves are not affected by Earth's rotation
- The polarization of *S* waves rotates in the same way as a Foucault pendulum
- The rotation of the *S* wave polarization is a manifestation of the Berry phase

Supporting Information:

- Supporting Information S1
- Figure S1
- Figure S2
- Figure S3
- Figure S4
- Figure S5
- Figure S6

Correspondence to:
R. Snieder,
rsnieder@mines.edu

Citation:
Snieder, R., C. Sens-Schönfelder, E. Ruigrok, and K. Shiomi (2016), Seismic shear waves as Foucault pendulum, *Geophys. Res. Lett.*, *43*, 2576–2581, doi:10.1002/2015GL067598.

Received 28 DEC 2015
Accepted 8 MAR 2016
Accepted article online 11 MAR 2016
Published online 29 MAR 2016

Seismic shear waves as Foucault pendulum

Roel Snieder[1,2], Christoph Sens-Schönfelder[2], Elmer Ruigrok[3,4], and Katsuhiko Shiomi[5]

[1]Center for Wave Phenomena, Colorado School of Mines, Golden, Colorado, USA, [2]GFZ German Research Centre for Geosciences, Potsdam, Germany, [3]Department of Earth Sciences, Utrecht University, Utrecht, Netherlands, [4]R&D Seismology and Acoustics, Royal Netherlands Meteorological Institute (KNMI), De Bilt, Netherlands, [5]National Research Institute for Earth Science and Disaster Prevention, Tsukuba, Japan

Abstract Earth's rotation causes splitting of normal modes. Wave fronts and rays are, however, not affected by Earth's rotation, as we show theoretically and with observations made with USArray. We derive that the Coriolis force causes a small transverse component for *P* waves and a small longitudinal component for *S* waves. More importantly, Earth's rotation leads to a slow rotation of the transverse polarization of *S* waves; during the propagation of *S* waves the particle motion behaves just like a Foucault pendulum. The polarization plane of shear waves counteracts Earth's rotation and rotates clockwise in the Northern Hemisphere. The rotation rate is independent of the wave frequency and is purely geometric, like the Berry phase. Using the polarization of *ScS* and *ScS*2 waves, we show that the Foucault-like rotation of the *S* wave polarization can be observed. This can affect the determination of source mechanisms and the interpretation of observed *SKS* splitting.

1. Introduction

Physical systems are affected by the rotation of the system. The imprint of rotation is described for classical mechanics [*Goldstein*, 1980], fluid mechanics [*Pedlosky*, 1992], electromagnetics [*Osmanov and Machabeli*, 2002], and quantum mechanics [*Xu and Tsai*, 1990; *Takagi*, 1991]. The imprint of rotation on elastic waves in anisotropic media is described by *Schoenberg and Censor* [1973], and it is known that Earth's rotation affects Earth's normal modes [*Backus and Gilbert*, 1961] and surface waves [*Tromp*, 1994]. The imprint of the Coriolis force on *PKP* travel times is discussed by *Maus* [2000] but was found to be negligible. In this work we elucidate the imprint of Earth's rotation on propagating shear waves.

We first discuss the imprint of rotation on the the direction of seismic waves (section 2) and show in section 3 the effect of Earth's rotation of propagating body waves. In section 4 we show observations of the change in polarization of shear waves by comparing the polarization of *ScS* and *ScS*2 waves that propagate under Japan. Details of the derivations and of the data analysis are shown in the supporting information.

2. Earth's Rotation and the Propagation of Rays

To introduce the imprint of Earth's rotation on seismic waves, we show the wavefield of the direct *P* wave recorded with USArray (http://www.usarray.org) after a deep earthquake in the Sea of Okhotsk in Figure 1a along with the great circle (green line) that connects the event with the center of the used stations. Beamforming of the direct *P* wave (Figure 1b) shows that these early arriving waves propagate along the great circle. Figure 1c shows the beamforming of the waves recorded between 8 and 9 h after the event; for this time window the waves that traveled multiple times through the Earth still arrive along the great circle. In 8 h, Earth rotates over 120°; a deflection of rays over this angle would be detectable as a rotation of the maxima in Figure 1c away from the great circle.

Figure 1c suggests that seismic rays are not deflected by the Coriolis force. To explain this, we investigate the imprint of Earth's rotation on seismic rays. We consider rays whose direction is denoted by the unit vector $\hat{\mathbf{n}}$. The equation of kinematic ray tracing is given by expression (4.44) of *Aki and Richards* [2002]: $d(\hat{\mathbf{n}}/c)/dl = \nabla(1/c)$, where c is the wave velocity and l the arclength along the ray. Using that $dl = c\,dt$ and defining the slowness in the unmoving medium as $\mathbf{S}_u = \hat{\mathbf{n}}/c$, the equation of kinematic ray tracing can be written as

$$\frac{d\mathbf{S}_u}{dt} = -S_u \nabla c \,, \tag{1}$$

with $S_u = 1/c$.

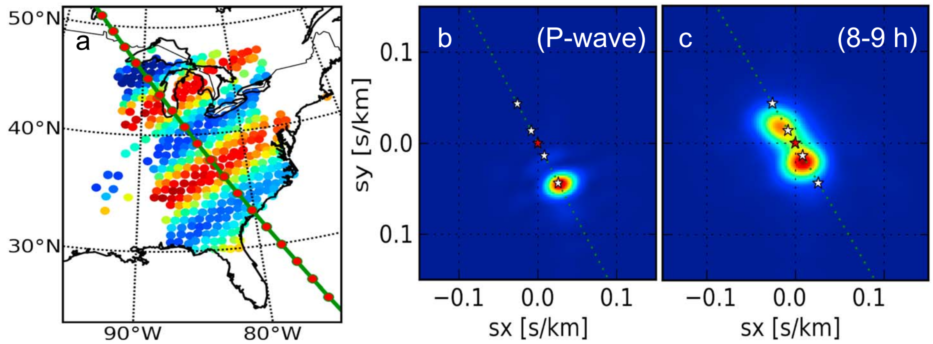

Figure 1. (a) Wavefield, bandpass filtered for periods between 32 s and 48 s recorded at USArray after a deep earthquake in the Sea of Okhotsk with the great circle pointing to the earthquake (green line). Beamforming of the wavefield recorded on the array for the direct (b) P wave and (c) the waves between 8–9 h after the event. The horizontal and vertical axes show slowness. Stars denote slowness of main body wave phases that propagate along the great circle.

We next consider a rotating Earth and analyze the equation of kinematic ray tracing in a coordinate system that does not rotate. In that fixed coordinate system, there is no Coriolis force, but the medium rotates with a velocity [*Snieder and van Wijk*, 2015]

$$\mathbf{V} = \mathbf{\Omega} \times \mathbf{r} \,, \tag{2}$$

where $\mathbf{\Omega}$ is Earth's rotation vector. According to expressions (8–1.5) and (8–1.10) of *Pierce* [1981], the equation of kinematic ray tracing in moving media is given by

$$\frac{d\mathbf{S}}{dt} = -S\nabla c - \mathbf{S} \times (\nabla \times \mathbf{V}) - (\mathbf{S} \cdot \nabla)\mathbf{V} \,, \tag{3}$$

where $\mathbf{S}$ now is the slowness perpendicular to the wavefront that includes the movement of the medium. For the rigid rotation (2), $\mathbf{S} \times (\nabla \times \mathbf{v}) + (\mathbf{S} \cdot \nabla)\mathbf{v} = -\mathbf{\Omega} \times \mathbf{S}$; hence, the equation of kinematic ray tracing is given by

$$\frac{d\mathbf{S}}{dt} = -S\nabla c + \mathbf{\Omega} \times \mathbf{S} \,, \tag{4}$$

The slowness vectors in expressions (1) and (4) are different because $\mathbf{S}$ includes the movement of the rotating Earth, while $\mathbf{S}_u$ does not. But the essential difference in these expressions is the term $\mathbf{\Omega} \times \mathbf{S}$; this term describes the corotation of the ray direction with Earth's rotation [*Goldstein*, 1980]. This corotation causes the rays to rotate with the Earth, which explains why after 9 h energy still propagates along the great circle (Figure 1c).

3. Earth's Rotation and the Polarization of Body Ways

But we know that Earth's rotation affects Earth's normal modes [*Backus and Gilbert*, 1961] and surface waves [*Tromp*, 1994]. This raises the question: what is the exact imprint of Earth's rotation on seismic body wave propagation? An account of body waves in general rotating elastic media is given by *Schoenberg and Censor* [1973]. Here we simplify the analysis for slowly rotating isotropic media. The fundamental mode of the Earth has a period of about 1 h; hence, $\Omega/\omega < 0.04$, with ω being the angular frequency of the wave motion. The following analysis is valid to first order in Ω/ω. We use a coordinate system with the z axis aligned with the direction of propagation and where the rotation vector $\mathbf{\Omega}$ lies in the $-y, z$ plane (Figure 2).

In the supporting information we solve the Christoffel equation in the presence of the Coriolis force using a time dependence $e^{-i\omega t}$. To first order in Ω/ω the P velocity is not changed: $c_P = \sqrt{(\lambda + 2\mu)/\rho} + O(\Omega/\omega)^2$, with λ and μ the Lamé parameters and ρ the density. The P wave has small transverse component:

$$\hat{\mathbf{q}}_P = \hat{\mathbf{z}} + \frac{2i}{\omega}\frac{\lambda + 2\mu}{\lambda + \mu}\,\hat{\mathbf{z}} \times \mathbf{\Omega} \,, \tag{5}$$

and the S wave has a small longitudinal component

$$q_{Sz} = \frac{2i\Omega \sin\theta}{\omega}\frac{\mu}{\lambda + \mu} \,, \tag{6}$$

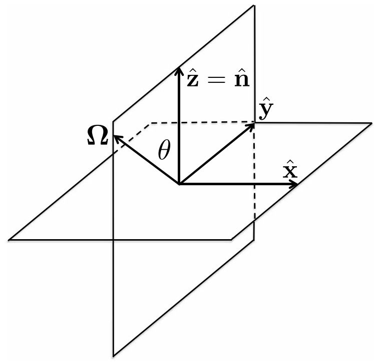

Figure 2. Definition of the unit vectors $\hat{\mathbf{x}}$, $\hat{\mathbf{y}}$, $\hat{\mathbf{z}}$, and the angle θ.

where θ is the angle between the direction of propagation $\hat{\mathbf{z}}$ and the rotation vector $\boldsymbol{\Omega}$. Both changes in the polarization are 90° out of phase with the usual polarization of *P* and *S* waves, which means that the polarization is slightly elliptical with ellipticity $\propto \Omega/\omega$. This anomalous polarization is caused by the sideways action of the Coriolis force, which is opposed by restoring elastic forces hence the dependence on the Lamé parameters.

The most significant imprint of Earth's rotation is on the transverse polarization of *S* waves; in the following we focus on this transverse polarization. We show in the supporting information that shear waves with time dependence $e^{-i\omega t}$ have two circular polarizations with opposite sense of rotation and different propagation velocities

$$\begin{aligned}\hat{\mathbf{q}}_{S+} &= \hat{\mathbf{x}} - i\hat{\mathbf{y}} \ \text{ with } \ c_S = c_S^{(0)}\left(1 + \frac{\Omega}{\omega}\cos\theta\right) , \\ \hat{\mathbf{q}}_{S-} &= \hat{\mathbf{x}} + i\hat{\mathbf{y}} \ \text{ with } \ c_S = c_S^{(0)}\left(1 - \frac{\Omega}{\omega}\cos\theta\right) ,\end{aligned} \tag{7}$$

with $c_S^{(0)} = \sqrt{\mu/\rho}$ the shear wave velocity in an unrotating system.

The shift in the shear velocity in expression (7) is similar to the frequency shift $\delta\omega_n$ of Earth's normal modes caused by the Coriolis force derived by *Backus and Gilbert* [1961] who show for toroidal modes that

$$\frac{\delta\omega_n}{\omega_n} = \frac{\Omega}{\omega_n}\frac{m}{l(l+1)} , \tag{8}$$

where ω_n is the normal mode frequency for mode *n*, while *l* and *m* are the angular order and degree, respectively. For spheroidal modes a similar expression holds, but the right-hand side contains a dimensionless constant that depends on the modal structure. The factor $m/l(l+1)$ in equation (8) plays the same role as $\cos\theta$ in expression (7), because *m* is the *z* component of the angular momentum of the spherical harmonics while $l(l+1)$ is the total angular momentum [*Merzbacher*, 1970].

The two shear waves with circular polarizations can be superposed to form a linear polarization. A perturbation δc_S in velocity corresponds to a perturbation $\delta k/k = -\delta c_S/c_S$ in wave number hence with expression (7)

$$\delta k = -\frac{\Omega\cos\theta}{\omega}k . \tag{9}$$

The superposition of the two circularly polarized shear waves is, using expressions (7) and (9), given by

$$\begin{aligned}\mathbf{u}(z,t) &= (\hat{\mathbf{x}} - i\hat{\mathbf{y}})\exp i\left(k\left(1 - \frac{\Omega\cos\theta}{\omega}\right)z - \omega t\right) \\ &+ (\hat{\mathbf{x}} + i\hat{\mathbf{y}})\exp i\left(k\left(1 + \frac{\Omega\cos\theta}{\omega}\right)z - \omega t\right) .\end{aligned} \tag{10}$$

Collecting terms multiplying $\hat{\mathbf{x}}$ and $\hat{\mathbf{y}}$, the expression above can be written as

$$\mathbf{u}(z,t) = \hat{\mathbf{q}}_S(z)e^{i(kz-\omega t)} , \tag{11}$$

with

$$\hat{\mathbf{q}}_S(z) = \hat{\mathbf{x}}\cos\left(\frac{k\Omega\cos\theta}{\omega}z\right) - \hat{\mathbf{y}}\sin\left(\frac{k\Omega\cos\theta}{\omega}z\right) . \tag{12}$$

This is a linearly polarized wave where the direction of the polarization vector is given by

$$\varphi = \arctan\left(q_y/q_x\right) = -\frac{k\Omega\cos\theta}{\omega}z\ . \tag{13}$$

The time derivative of the location of the wavefronts is given by

$$\dot{z} = c_S = \omega/k\ . \tag{14}$$

Using this in the time derivative of expression (13) implies that the rate of rotation of the polarization of the *S* waves in the transverse plane is given by

$$\dot{\varphi} = -\Omega\cos\theta\ . \tag{15}$$

The minus sign means that the polarization of the *S* wave rotates in the opposite direction as Earth's rotation. The projection of the rotation vector along the direction of propagation is $\Omega\cos\theta$, which is the rotation rate of Foucault's pendulum [*Pérez and Pujol*, 2015]. As shown by equation (15) this rotation is exactly compensated by the rotation of the polarization vector in the plane perpendicular to the direction of wave propagation. The rate of change of the *S* wave polarization vector follows from expressions (12) and (14) and is given by

$$\dot{\hat{\mathbf{q}}}_S = -\Omega\cos\theta\ \hat{\mathbf{z}}\times\hat{\mathbf{q}}_S\ . \tag{16}$$

This amounts to a rotation in the (x, y) plane with a rotation vector $-\Omega\cos\theta\ \hat{\mathbf{z}}$. This means that shear waves behave exactly like a Foucault pendulum [*Pérez and Pujol*, 2015], as the change of the polarization plane caused by Earth's rotation is the same as for Foulcault's pendulum. An elliptically polarized shear wave can be written as the superposition of two linearly polarized shear waves that are 90° out off phase. Each of the linear shear wave polarizations rotates with the same rotation rate (15), and hence, the elliptical polarization rotates with the same rate. Expressions (15) and (16) therefore are applicable to elliptically polarized shear waves as well.

The circular polarizations in expression (7) have a direct analog in the Bravais pendulum [*Babović and Mekić*, 2011]. Just as the Foucault pendulum, the Bravais pendulum consists of a mass that is suspended by a long thin wire. In Foucault's pendulum the mass oscillates in a plane, while in the Bravais pendulum the mass moves in a circular orbit, either in the clockwise or in the counterclockwise direction. When this orbit moves against Earth's rotation, it takes less time to move over a full circle than when it moves with Earth's rotation. The difference in the orbit times for the two circular motions of the mass can be used to measure Earth's rotation.

The rotation rate of the *S* wave polarization is independent of the wave frequency and is thus a purely geometric effect resulting from parallel transport along a 3-D path, as it is for Foucault's pendulum [*Pérez and Pujol*, 2015]. It is similar to geometric phases like the Berry phase [*Berry*, 1984] observed in optics and quantum physics. A straight segment of a seismic ray in the rotating system corresponds, due to Earth's rotation, with a segment of a helix in a nonrotating system. The resulting geometric phase is the same as if the helix-like shape of the ray was enforced by the structure of a nonrotating medium, e.g., in a helical spring [*Boulanger et al.*, 2012].

4. Observations of the Change in Polarization of *S* Waves

Detecting the change in polarization for *S* waves due to Earth's rotation is challenging because during propagation of the main *S* wave phases (about 30 min) Earth rotates only over about 7°. We study the change in polarization between *ScS* and *ScS*2 waves that have bounced once or twice off the core-mantle boundary. For steeply propagating *ScS* waves, the change in polarization due to Earth' rotation for each bounce at colatitude $\theta = 55°$ is $\Delta\varphi_{\rm rot} = -\Omega t\cos\theta = -2.26°$ for a travel time t=940 s. We use tiltmeter records of Hi-net, a seismic network in Japan (Figures 3a and 3b) for two earthquakes. The western event is the M_w=6.2 Tanegashima earthquake (21 November 2005, depth = 150 km) and the eastern event is the M_w=7.2 Miyagi earthquake (16 August 2005, depth = 40 km).

We use earthquakes on both sides of the array for the following reason. The change in polarization φ is caused by a contribution $\varphi_{\rm rot}$ due to Earth's rotation and a contribution $\varphi_{\rm struc}$ due to ray bending by laterally

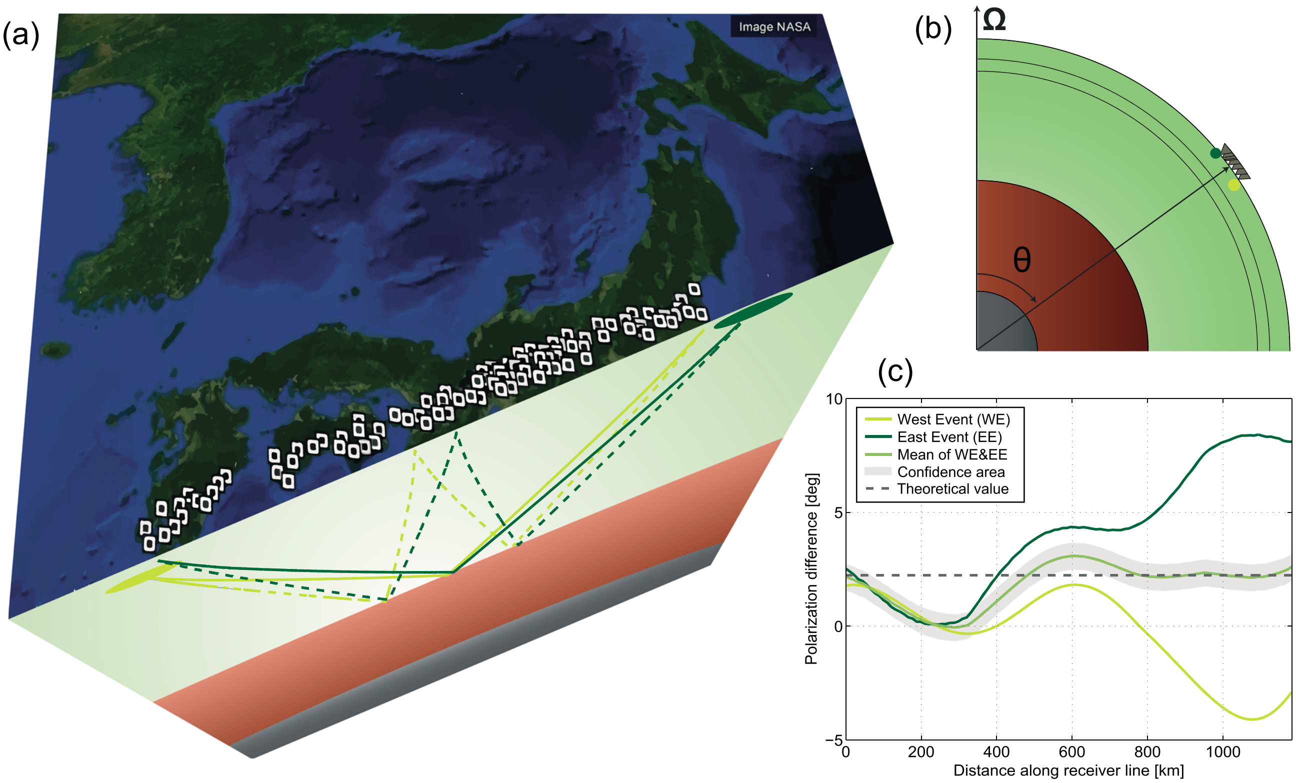

Figure 3. (a) Geometry of the earthquakes (yellow and dark green circles) and stations (squares), with ray paths for *ScS* (solid lines) and *ScS*2 (dashed lines) between each earthquake and the furthest station within the array. The mantle is indicated by the green area and the outer core by the red area. The vertical scale is compressed, and the rays propagate in the near-vertical direction. The distance between the *ScS*2 bounce points at the surface is less than 100 km. (b) Vertical cross section in north-south direction. (c) The change in *S* wave polarization between *ScS*2 and *ScS* waves for the west event (yellow) and the east event (dark green) and their average ($\mu(x)$, light green) as a function of epicentral distance from each event, along with the theoretical value (dashed line). The grey shaded area denotes the region bounded by $\mu(x) \pm \sigma$. The determination of the standard deviation σ is discussed in the supporting information.

varying Earth structure. We show in the supporting information that for a horizontal velocity gradient in the upper mantle of 1%/200 km, the resulting change in the polarization direction is about 2°, which is comparable to the change in polarization caused by Earth's rotation. It follows from time reversal invariance that the structure-induced rotation of polarization for rays propagating in opposite directions is opposite. This also follows from expression (4.1.5) of *Červený* [2001]. For Earth's rotation, the change in polarization is in the same clockwise direction on the Northern Hemisphere regardless of the direction of propagation. Another way to state this is that the imprint of velocity structure is invariant for time reversal, while that of rotation is not (unless one changes the rotation vector as well). Hence, for waves propagating in opposite directions with polarization change $\varphi_{\pm}$, respectively, $\varphi_{\pm} = \varphi_{\rm rot} \pm \varphi_{\rm struc}$, hence

$$\varphi_{\rm rot} = (\varphi_{+} + \varphi_{-})/2 \,. \qquad (17)$$

Averaging the change in polarization for waves propagating in opposite directions thus removes the imprint of lateral velocity variations.

The data processing involves frequency filtering (periods 50–100 s), correcting the *SV* motion for the reflection coefficients at Earth's surface and the core mantle boundary so that the *SH* waves and corrected *SV* waves are both completely reflected, alignment of the arriving waves, and f, k-filtering (supporting information). The resulting change in polarization between the *ScS2* and *ScS* arrivals is shown in Figure 3c for the eastern event (dark green line) and the western event (yellow line) as a function of epicentral distance. The polarization in the data is measured clockwise from the great circle direction at each station. These polarization differences are due to a combination of lateral velocity variations and Earth's rotation. For short distances along the receiver line (x<700 km) the rays sample different parts of the mantle, and the change in polarization is masked by the imprint of earth structure. As the distance approaches 1200km, the rays sample the same region (Figure 3a). The imprint of horizontal variations in Earth structure on polarization is opposite, and the mean of the polarization differences for the two events, ($\mu(x)$, light green curve in Figure 3c), is for the larger distances not equal to zero but is close to the change in polarization caused by earth rotation (2.26°). This estimated change in polarization is 3.8 times as large as the standard deviation (0.59°).

5. Conclusion

The observed change in *S* wave polarization between *ScS*2 waves and *ScS* waves agrees with the change predicted by expression (15). This is an experimental confirmation that *S* waves in the Earth behave as a Foucault pendulum. Alternatively, one can view our observation of the change in *S* wave polarization caused by Earth's rotation as a seismic manifestation of the Berry phase [*Pérez and Pujol*, 2015; *Berry*, 1984].

For typical observations of body waves the rotation effect is small because Earth does not rotate much over the propagation time of *S* waves in the Earth (2.5° in 10 min). The change in polarization due to Earth's rotation should be considered in high precision investigations that rely on polarization, such as the determination of source mechanisms from *S* wave polarizations. In elastic anisotropic media shear wave splitting may occur, leads to an elliptical polarization of the *S* waves, and the orientation of the polarization with the highest velocity provides information on azimuthal anisotropy [*Vinnik et al.*, 1989; *Silver and Chan*, 1991]. Since an elliptically polarized shear wave also rotates with the rotation rate (15), *SKS* splitting measurements are affected by Earth's rotation as well. Our analysis provides a simple formula to estimate, and potentially correct for, the Foucault-like rotation of the polarization direction. Our work makes it possible to measure the change in polarization $\varphi_{\rm struc}$ due to Earth structure. Measurements of this quantity could be used to constrain the horizontal velocity gradients in the Earth. Using cylindrical resonators of materials with low attenuation, one can, in principle, build rotational sensors that measure the rate of change of *S* wave polarizations or toroidal modes to measure the projection of the rotation vector along the axis of the cylinder.

Acknowledgments
We thank two anonymous reviewers, Frederik Tilmann and Oleg Godin, for their comments and Kiwamu Nishida for assistance in the data preparation. Roel Snieder was supported by the Alexander von Humboldt Foundation. The data used in this study can be obtained from NIED Japan by sending a request to hinet-admin@bosai.go.jp. The authors have no financial interest in this work.

References

Aki, K., and P. Richards (2002), *Quantitative Seismology*, 2nd ed., 700 pp., Univ. Science Books, Sausalito.
Babović, V., and S. Mekić (2011), The Bravais pendulum: The distinct charm of an almost forgotten experiments, *Eur. J. Phys.*, *32*, 1077–1086.
Backus, G., and F. Gilbert (1961), The rotational splitting of the free oscillations of the earth, *Proc. Natl. Acad. Sci.*, *47*, 362–371.
Berry, M. (1984), Quantal phase factors accompanying adiabatic changes, *Proc. R. Soc. Lon. A*, *392*, 45–57.
Boulanger, J., N. Le Bihan, S. Catheline, and V. Rosetto (2012), Obervations of a non-adiabatic geometric phase for elastic waves, *Ann. Phys.*, *327*, 952–958.
Červený, V. (2001), *Seismic ray theory*, Cambridge Univ. Press, Cambridge, U. K.
Goldstein, H. (1980), *Classical Mechanics*, 2nd ed., 672 pp., Addison-Wesley, Reading, Mass.
Maus, S. (2000), Is there an observable lack of reciprocity in PKP(DF) traveltimes?, *Geophys. J. Int.*, *143*, 274–277.
Merzbacher, E. (1970), *Quantum Mechanics*, 2nd ed., Wiley, New York.
Osmanov, Z., and G. Machabeli (2002), Electromagnetic waves in a rigidly rotating frame, *Phys. Rev. A*, *66*, 042103.
Pedlosky, J. (1992), *Geophysical Fluid Dynamics*, 2nd ed., Springer, New York.
Pérez, J.-P., and O. Pujol (2015), Two often disregarded aspects of Foucault's pendulum, *Eur. J. Phys.*, *36*, 015019.
Pierce, A. (1981), *Acoustics, An Introduction to Its Physical Principles and Applications*, McGraw-Hill, New York.
Schoenberg, M., and D. Censor (1973), Elastic waves in rotating media, *Quartely of Appl. Math.*, *31*, 115–125.
Silver, P., and W. Chan (1991), Shear wave splitting and subcontinental mantle deformation, *J. Geophys. Res.*, *96*, 16,429–16,454.
Snieder, R., and K. van Wijk (2015), *A Guided Tour of Mathematical Methods for the Physical Sciences*, 3rd ed., 560 pp., Cambridge Univ. Press, Cambridge, U. K.
Takagi, S. (1991), Quantum dynamics and non-inertial frames of reference. I, *Prog. Theor. Phys.*, *85*, 463–479.
Tromp, J. (1994), Surface-wave propagation on a rotating, anisotropic earth, *Geophys. J. Int.*, *117*, 141–152.
Vinnik, L., V. Farra, and B. Romanowicz (1989), Azimuthal anisotropy in the Earth from observations of SKS at GEOSCOPE and NARS broadband stations, *Bull. Seism. Soc. Am.*, *79*, 1542–1558.
Xu, H.-H., and C.-H. Tsai (1990), Quantum interference in general rotating systems, *Phys. Rev. A*, *41*, 4046–4048.